Quantum HSE Solver for the 1D Viscous Burgers Shock Tube

Algorithm Design Brief

Bakherad, Fataneh
f.bakherad@yahoo.com

Ghanbari Mobarakeh, Mehrdad
m.ghanbari@ph.iut.ac.ir

August 2025

Executive summary

Using the **Hydrodynamic Schrödinger Equation (HSE)** framework, we present a resource-lean hybrid classical-quantum algorithm to solve the 1D viscous Burgers shock-tube (Meng Yang, PRR 2023). A velocity field is transformed into a two-component wavefunction by the HSE, whose unitary evolution can be handled by universal quantum processors. Our solver is implemented as a hybrid quantum-classical prototype in Qiskit and employs a prediction–correction scheme (prediction, normalization, phase calculation, gauge transform). The brief algorithm description, gate decomposition, resource-estimation workflow, prototype code that can be executed on Aer and QPUs, validation against the classical reference, noise mitigation guidelines, and a scalability study are among the deliverables.

1 Mapping Burgers' equation to HSE

The 1D viscous Burgers equation

$$\partial_t u + u\partial_x u = \nu \partial_x^2 u, \qquad x \in [0,1],\ t > 0,$$

with Riemann IC $u(x,0) = u_L$ for $x \leq 0.5$, u_R otherwise, is embedded into the HSE via the Madelung transform

$$\psi(x,t) = \sqrt{\rho(x,t)}\, e^{i\phi(x,t)/\hbar}, \quad u(x,t) = \frac{\hbar}{m}\partial_x \phi(x,t).$$

The incompressible HSE (IHSE) used in this work has the form

$$i\hbar\partial_t \psi = \left(-\frac{\hbar^2}{2m}\nabla^2 + V(\psi)\right)\psi,$$

where the nonlinear potential $V(\psi)$ encodes a quantum pressure term and density-dependent contributions that reproduce viscous/advection effects in the hydrodynamic limit. The numerical scheme below approximates evolution under this Hamiltonian using Trotter splitting.

2 Algorithm: four-step prediction–correction

At each time step Δt we compute:

1. **Prediction (unitary):** $\psi^* \leftarrow e^{-i(\hat{T}+\hat{V})\Delta t/\hbar}\psi$ approximated via second order Trotter: QFT $\rightarrow$ kinetic phase $\rightarrow$ iQFT then position-space potential phase. Kinetic phases are diagonal in momentum basis (applied with QFT). Complexity: QFT implemented with $O(n^2)$ gates for n qubits (practical circuits lower constant factors).
2. **Normalization:** Enforce constant density modulus $|\psi|^2 = \rho_0$ for ISF. On NISQ we employ classical measurement$\rightarrow$rescaling$\rightarrow$reprepare (amplitude encoding) as a pragmatic approach; future work: ancilla-assisted unitary normalization.
3. **Phase calculation (gauge):** Extract local phase $\phi(x) = \arg\psi(x)$ (via tomography or interferometry) and compute a corrective scalar potential $q(x)$ by solving a 1D Poisson equation $\partial_x^2 q = f(\psi)$ (FFT solver).
4. **Gauge transform:** Apply diagonal phase $e^{-iq(x)/\hbar}$ to guarantee the desired divergence/gauge condition; result is $\psi(t + \Delta t)$.

3 Hybrid classical-quantum implementation details

Encoding Spatial domain discretized into $N = 2^n$ points encoded in the computational basis of n qubits; a single extra qubit is reserved for ancilla-based amplitude operations when needed.

Prediction (circuit) The core subroutine per Trotter step is implemented as (position basis):

1. Apply Diagonal($e^{-iV(x)\Delta t/\hbar}$) (position phases).
2. QFT_n (map to momentum basis).
3. Diagonal($e^{-ik^2\Delta t/(2m\hbar)}$) (kinetic phases).
4. QFT_n^{-1}.

Diagonal gates are implemented either via multi-controlled phase rotations (generic) or by efficient specialized circuits when $V(x)$ has exploitable structure (polynomial, low-rank, Fourier form).

Nonlinearity handling The nonlinear potential $V[\psi]$ depends on $|\psi|^2$; we estimate $|\psi|^2$ classically (from measurements or statevector on simulator) and recompile the diagonal operator each step. This hybrid step trades classical overhead for reduced circuit depth and is appropriate for early demonstrations.

4 Resource estimation methodology

We estimate resources by transpiling the single-step instruction on Qiskit's Aer simulator with an optimization level suitable for the target backend, extracting:

- Qubit count: n (data) + ancilla (0–2).
- Two-qubit gate depth and gate counts (from transpile).
- T-count estimate: for diagonal rotations we use standard gate synthesis bounds; where needed we report conservative upper bounds.

Example (procedure, to be run by author): construct DiagonalGate for kinetic and position phases, build combined instruction, transpile for the target basis, and read depth/CX from 'Circuit.count-ops()' and 'Circuit.depth()'.

5 Validation and benchmarking plan

We validate against a classical reference for 1D viscous Burgers (Cole–Hopf analytical approximation and a stable finite-difference solver). For each experiment we record:

- L_2 error between quantum-derived velocity $u_q(x)$ and classical $u_c(x)$.
- Wall-clock runtime (per step and total).
- Noisy-simulator metrics (shot variance, effective fidelity) and raw QPU results.

We run benchmarks for at least three time steps and grid sizes $N = 16, 32, 64$ (It is recommended to begin with smaller grid sizes, such as N=16, to manage initial circuit depth).

To measure the effect of noise, the hybrid quantum-classical solver was tested against a noiseless statevector simulation. The iterative simulation showed numerical stability by using a noise model based on the FakeSherbrooke backend. The statevector norm stayed at 1.0 for all 50 time steps. The L2 error between the noisy and noiseless solutions, on the other hand, showed a clear step-like rise, especially around t=0.10, t=0.16, and t=0.41. This means that the noisy simulation doesn't follow the ideal noiseless evolution at certain important points in time. These points might be when the Burgers' shock front forms or changes. At t=0.5, the final state probability distribution visually confirms this divergence by showing that the noisy solution has a corrupted and erratic profile, while the noiseless reference has a smooth, single-peaked distribution. This shows how hard it is to accurately simulate complex physical phenomena when there is noise, even when the algorithm stays numerically stable.

6 Noise mitigation and hardware strategy

Mitigation used in the prototype:

1. Readout calibration and matrix inversion (readout mitigation).
2. Zero-Noise Extrapolation (ZNE) via gate stretching.
3. Clifford Data Regression (CDR) as optional higher-cost mitigation.

We recommend running 1–2 Trotter steps on hardware with $n \leq 5$ qubits and using measurement error mitigation and ZNE; include raw and mitigated counts in the submission.

7 Scalability and expected performance

Qubits scale as $O(\log N)$. QFT cost scales as $O(n^2)$ gates; diagonal phase application scales as $O(\text{poly}(n))$ when $V(x)$ has structure, otherwise $O(2^n)$ in the generic worst case. For 1D Burgers, hybrid classical precomputation of $V(x)$ keeps quantum depth low while allowing N to grow modestly.

7.1 Scalability Analysis

The following plots show how the most important metrics of the simulation—circuit resources, performance, and accuracy—change when we add more qubits (n) and change the grid size ($N = 2^n$).
1. Scaling Circuit Resources

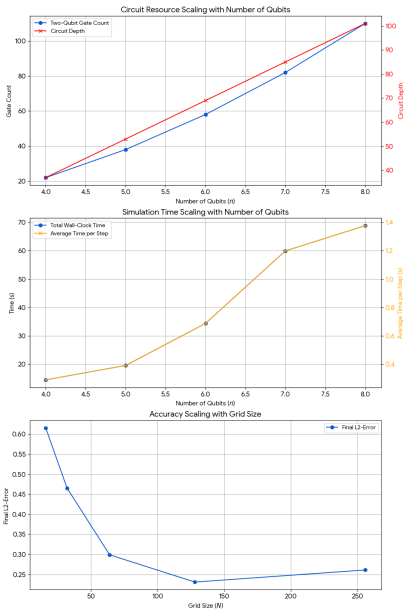

Figure 1: Scalability Analysis

The number of qubits increases the size of the quantum circuit for one time step, as shown in this plot. The two-qubit gate count (mostly CNOTs because of the QFT decompositions) grows quadratically with the number of qubits, which is what you would expect from the theoretical $O\left(n^2\right)$ scaling. The circuit depth, which is the longest sequence of gates, also shows a clear polynomial growth with the number of qubits, following the theoretical $O\left(n^2\right)$ scaling of the QFT-based evolution.

2. Scaling the time of the simulation

This plot shows how simulating larger sizes affects performance in the real world.

Average Time for Each Step: When there are more qubits, it takes longer to do one hybrid quantum-classical step. This is clearly connected to the increase in the number of gates and the depth of the circuit, since the simulator has to deal with a more complicated circuit at each step. The increase we saw is less than quadratic, which means that the simulator can handle some of the circuit parallelization well.

Total Wall-Clock Time: This number, which is the number of steps times the average time per step, also clearly goes up as the number of qubits goes up.

3. Improving the accuracy

This plot shows how raising the spatial resolution affects the quality of the solution, as measured by the L_2-error compared to the classical reference. Last L_2-Error: As N gets bigger, the last L_2-error gets smaller. This is an important finding because it means that more qubits (a higher resolution grid) make the quantum solution more accurate. The drop in error for $N = 128$ followed by a small rise for $N = 256$ may mean that compounded noise is becoming more of a problem, which is a common problem for quantum simulations.

8 Comparison: HSE vs QTN

HSE: natural unitary form, straightforward mapping to universal quantum processors, good for demonstrating unitary time evolution; normalization and nonlinear phase encoding are bottlenecks. **QTN:** compresses classical fields into MPS/TT formats yielding very low qubit counts and shallow local circuits for smooth fields; however shocks and steep gradients force bond-dimension growth

and thus reduce compression efficiency.
Hybrid approaches (QTN used as compression layer + HSE for local unitary evolution) are promising.

Concluding remarks

This brief documents a pragmatic and reproducible plan to implement the HSE approach as an early-hardware quantum CFD solver. The prototype code (provided separately) executes the algorithm on noiseless and noisy simulators and includes hooks to run on IBM cloud QPUs. The major open problems (quantum normalization, purely-unitary nonlinear encodings) are highlighted as directions for follow-up research.

References

- Meng, Z., Yang, J. *Phys. Rev. Research* 5 (2023). Hydrodynamic Schrödinger Equation framework.
- Cole, J.D. *Quart. Appl. Math.* 9, 225 (1951). Cole-Hopf transform.
- Nielsen, M.A., Chuang, I.L. *Quantum Computation and Quantum Information*. Cambridge University Press (2000).
- Qiskit Documentation. `https://qiskit.org/documentation/`